

# Non-Reversible Langevin Algorithms for Constrained Sampling

Hengrong Du<sup>1</sup>, Qi Feng<sup>2</sup>, Changwei Tu<sup>3</sup>, Xiaoyu Wang<sup>4</sup>, Lingjiong Zhu<sup>5</sup>

January 22, 2025

## Abstract

We consider the constrained sampling problem where the goal is to sample from a target distribution on a constrained domain. We propose skew-reflected non-reversible Langevin dynamics (SRNLD), a continuous-time stochastic differential equation with skew-reflected boundary. We obtain non-asymptotic convergence rate of SRNLD to the target distribution in both total variation and 1-Wasserstein distances. By breaking reversibility, we show that the convergence is faster than the special case of the reversible dynamics. Based on the discretization of SRNLD, we propose skew-reflected non-reversible Langevin Monte Carlo (SRNLMC), and obtain non-asymptotic discretization error from SRNLD, and convergence guarantees to the target distribution in 1-Wasserstein distance. We show better performance guarantees than the projected Langevin Monte Carlo in the literature that is based on the reversible dynamics. Numerical experiments are provided for both synthetic and real datasets to show efficiency of the proposed algorithms.

## 1 Introduction

We consider the problem of sampling a distribution  $\pi$  on a convex constrained domain  $\mathcal{C} \subsetneq \mathbb{R}^d$  with probability density function

$$\pi(x) \propto \exp(-f(x)), \quad x \in \mathcal{C}, \quad (1.1)$$

for a function  $f : \mathbb{R}^d \rightarrow \mathbb{R}$ . The sampling problem for both constrained domain  $\mathcal{C} \subsetneq \mathbb{R}^d$  and unconstrained domain  $\mathcal{C} = \mathbb{R}^d$  is a fundamental problem that arises in many applications, including Bayesian statistical inference [GCSR95], Bayesian formulations of inverse problems [Stu10], as well as Bayesian classification and regression tasks in machine learning [ADFDJ03, TTV16, GGHZ21, GHZ24, GIWZ24].

---

<sup>1</sup>Department of Mathematics, University of California, Irvine, 410P Rowland Hall, Irvine, CA 92697-3875, United States of America; hengrond@uci.edu

<sup>2</sup>Department of Mathematics, Florida State University, 1017 Academic Way, Tallahassee, FL-32306, United States of America; qfeng2@fsu.edu

<sup>3</sup>Hong Kong University of Science and Technology (Guangzhou), Guangzhou, Guangdong Province, People's Republic of China; ctu570@connect.hkust-gz.edu.cn

<sup>4</sup>Hong Kong University of Science and Technology (Guangzhou), Guangzhou, Guangdong Province, People's Republic of China; xiaoyuwang@hkust-gz.edu.cn

<sup>5</sup>Department of Mathematics, Florida State University, 1017 Academic Way, Tallahassee, FL-32306, United States of America; zhu@math.fsu.edu

In the literature, [BEL15, BEL18] studied the projected Langevin Monte Carlo (PLMC) algorithm for constrained sampling that projects the iterates back to the constraint set after applying the Langevin step:

$$x_{k+1} = \mathcal{P}_{\mathcal{C}} \left( x_k - \eta \nabla f(x_k) + \sqrt{2\eta} \xi_{k+1} \right), \quad (1.2)$$

where  $\mathcal{P}_{\mathcal{C}}$  is the projection onto the set  $\mathcal{C}$ ,  $\eta > 0$  is the stepsize,  $\xi_k$  are i.i.d. Gaussian random vectors  $\mathcal{N}(0, I)$  and the dynamics (1.2) is based on the continuous-time overdamped Langevin stochastic differential equation (SDE) with reflected boundary:

$$dX_t = -\nabla f(X_t)dt + \sqrt{2}dW_t + \nu(X_t)L(dt), \quad (1.3)$$

where the term  $\nu(X_t)L(dt)$  ensures that  $X_t \in \mathcal{C}$  for every  $t$  given that  $X_0 \in \mathcal{C}$ . In particular,  $\int_0^t \nu(X_s)L(ds)$  is a bounded variation reflection process and the measure  $L(dt)$  is such that  $L([0, t])$  is finite,  $L(dt)$  is supported on  $\{t | X_t \in \partial\mathcal{C}\}$ .

It is shown in [BEL18] that  $\tilde{\mathcal{O}}(d^{12}/\varepsilon^{12})$  iterations are sufficient for having  $\varepsilon$ -error in the total variation (TV) distance with respect to the target distribution when the gradients are exact where the notation  $\tilde{\mathcal{O}}(\cdot)$  hides some logarithmic factors. [Lam21] considers the projected stochastic gradient Langevin dynamics in the setting of non-convex smooth Lipschitz  $f$  on a convex body where the gradient noise is assumed to have finite variance with a uniform sub-Gaussian structure. The author shows that  $\tilde{\mathcal{O}}(d^4/\varepsilon^4)$  iterations suffice in the 1-Wasserstein metric; see also [ZL22]. In addition, proximal Langevin Monte Carlo is proposed for constrained sampling and a complexity of  $\tilde{\mathcal{O}}(d^5/\varepsilon^6)$  is obtained. [SR20] further studies the proximal stochastic gradient Langevin algorithm from a primal-dual perspective. Mirror descent-based Langevin algorithms (see e.g. [HKRC18, CLGL<sup>+</sup>20, ZPFP20, LTVW22, AC21]) can also be used for constrained sampling. Mirrored Langevin dynamics was proposed in [HKRC18], inspired by the classical mirror descent in optimization. Very recently, inspired by the penalty method in the optimization literature, penalized Langevin Monte Carlo algorithms are proposed and studied in [GHZ24], where the objective  $f$  can be non-convex in general, and the better dependency on the dimension  $d$  is achieved in the complexity compared to the previous literature.

In the literature, non-reversible Langevin SDE and the associated algorithms (supported on  $\mathbb{R}^d$ ) have been studied and are known to converge to the Gibbs distribution faster than the overdamped Langevin SDEs and algorithms. This motivates us to investigate whether non-reversibility can help in the context of projected Langevin for constrained sampling. In particular, by adding a (state-dependent) *anti-symmetric* matrix  $J = -J^\top$  to the overdamped Langevin diffusion, a non-reversible Langevin SDE takes the form:

$$dX_t = -(I + J(X_t))\nabla f(X_t)dt + \sqrt{2}dW_t, \quad (1.4)$$

where  $W_t$  is a standard  $d$ -dimensional Brownian motion, then the stationary distribution has the density  $\pi(x) \propto e^{-f(x)}$  which is the same as the Gibbs distribution of the overdamped Langevin. This dynamics is called *non-reversible Langevin dynamics* (NLD) because this diffusion is a non-reversible Markov process due to the addition of the  $J$  matrix whereas the overdamped Langevin

diffusion is reversible (see [HHMS93a, HHMS05] for details) with optimal choice of  $J$  discussed in [LNP13a, WHC14]. The main idea explored here is that non-reversible processes converge to their equilibrium often faster than their reversible counterparts [HHMS93a, HHMS05] and this has been applied to sampling [RBS16, DLP16, RBS15b, DPZ17, RBS15a, FSS20] and non-convex optimization [GGZ20, HWG<sup>+</sup>20].

In this paper, we introduce the *skew-reflected non-reversible Langevin dynamics* (SRNLD):

$$dX_t = -(I + J(X_t))\nabla f(X_t)dt + \sqrt{2}dW_t + \nu^J(X_t)L(dt), \quad (1.5)$$

where for every  $x$ ,  $J(x)$  is an anti-symmetric matrix, i.e.  $J(x) = -(J(x))^\top$  and  $\|J\|_\infty := \sup_{x \in \mathcal{C}} \|J(x)\| < \infty$ . The term  $\nu^J(X_t)L(dt)$  ensures that  $X_t \in \mathcal{C}$  for every  $t$  given that  $X_0 \in \mathcal{C}$ .

In particular,  $\int_0^t \nu^J(X_s)L(ds)$  is a bounded variation *skew-reflection* process and the measure  $L(dt)$  is such that  $L([0, t])$  is finite,  $L(dt)$  is supported on  $\{t | X_t \in \partial\mathcal{C}\}$ , where the skew-reflection is defined through the following *skew unit normal vector*:

$$\nu^J(X_t) = \frac{(I + J(X_t))\nu(X_t)}{\sqrt{\|\nu(X_t)\|^2 + \|J(X_t)\nu(X_t)\|^2}}, \quad (1.6)$$

where  $\nu(X_t) \in \mathcal{N}_{\mathcal{C}}(X_t)$  is referring to the unit inner normal vector, and we denote  $\mathcal{N}_{\mathcal{C}}(x)$  as the normal cone of  $\mathcal{C}$  at  $x$ . We assume the skew-matrix  $J$  satisfies the condition that  $\langle \nu^J, \nu \rangle \geq \delta_0 > 0$  for some positive constant  $\delta_0$ . Under these conditions, the reflection process is uniquely defined. The skew-reflection  $\nu^J$  introduced here in (1.6) is different from [BEL18] due to the non-reversible dynamics (1.4). In the literature, stochastic differential equations with reflection and oblique reflection have been studied in [Tan79, LS84, Cos92, BGT04]. However, to the best of our knowledge, the invariant distribution of oblique reflection processes and their exponential convergence to the invariant distribution have not been studied. The newly proposed reflection is compatible with the boundary condition and keeps the invariant measure of (1.4) unchanged. To be precise, the skew-reflection is realized through the following procedures. Define the projection  $\mathcal{P}_{\mathcal{C}}$  and reflection  $\mathcal{R}_{\mathcal{C}}$  as below,

$$\mathcal{P}_{\mathcal{C}}(x) := \operatorname{argmin}_{y \in \bar{\mathcal{C}}} \|y - x\|, \quad \mathcal{R}_{\mathcal{C}}(x) := 2\mathcal{P}_{\mathcal{C}}(x) - x. \quad (1.7)$$

We then define the following skew-reflection:

$$\mathcal{R}_{\mathcal{C}}^J(x) := (I + J(x))(\mathcal{P}_{\mathcal{C}}(x) - x) + \mathcal{P}_{\mathcal{C}}(x). \quad (1.8)$$

Motivated by such a skew-reflection, we propose the following *skew-projection*:

$$\mathcal{P}_{\mathcal{C}}^J(x) := \operatorname{argmin}_{y \in \bar{\mathcal{C}}} \langle y - x, \nu^J(\mathcal{P}_{\mathcal{C}}(x)) \rangle. \quad (1.9)$$

Observe that we have  $x - \mathcal{P}_{\mathcal{C}}^J(x)$  parallel to  $\mathcal{R}_{\mathcal{C}}^J(x) - \mathcal{P}_{\mathcal{C}}(x)$ . To implement SRNLD (1.5), in practice, we propose the *skew-reflected non-reversible Langevin Monte Carlo* (SRNLMC) algorithm:

$$x_{k+1} = \mathcal{P}_{\mathcal{C}}^J \left( x_k - \eta(I + J(x_k))\nabla f(x_k) + \sqrt{2\eta}\xi_{k+1} \right), \quad (1.10)$$

where  $\xi_k$  are i.i.d. Gaussian random vectors  $\mathcal{N}(0, I)$ . In particular, when  $J(\cdot) \equiv 0$ , the algorithm SRNLMC (1.10) reduces to the projected Langevin Monte Carlo algorithm (PLMC) in the literature [BEL15, BEL18]; When  $J(\cdot) \neq 0$ , the skew-reflected algorithm is equivalent to the skew projection onto the boundary  $\partial\mathcal{C}$  parallel to  $\nu^J$ ; see [BGT04][Proposition 1].

In this paper, we are interested in studying the continuous-time SRNLD (1.5) including the non-asymptotic convergence performance, as well as the discretization error of the discrete-time algorithm, SRNLMC (1.10), that approximates (1.5), which yields iteration complexities for (1.10). Our contributions can be stated as follows:

- We propose SRNLD, a continuous-time non-reversible Langevin SDE on a constrained domain. This includes the reversible Langevin SDE on a constrained domain in the literature as a special case [BEL15, BEL18, Lam21]. Our technical novelty lies upon the construction of a skew-reflected boundary and the establishment of the well-posedness of the non-reversible Langevin SDE with a skew-reflected boundary. First, we show the existence of the Skorokhod problem (Lemma 2.3). Next, we show that SRNLD admits the Gibbs distribution as an invariant distribution (Theorem 2.6). Moreover, we obtain non-asymptotic convergence rate for continuous-time SRNLD in TV and 1-Wasserstein distances to the Gibbs distribution (Theorem 2.11). We allow the target distribution to be non-convex, and our assumption is weaker than even the special case of the reversible reflected Langevin SDE in the literature [BEL15, BEL18, Lam21]. Furthermore, by breaking reversibility, we show that the non-reversible SRNLD has better convergence rate compared to the reversible reflected Langevin SDE in the literature (Theorem 2.11).
- Moreover, we provide non-asymptotic discretization error in 1-Wasserstein distance for the discrete-time algorithm SRNLMC that keeps track of the continuous-time SRNLD (Corollary 2.19). In particular, by combining with our non-asymptotic analysis for the continuous-time SRNLD (Theorem 2.11), this yields the iteration complexity for SRNLMC algorithm in 1-Wasserstein distance (Theorem 2.20, Corollary 2.21), better than PLMC algorithm in the literature that is based on the reversible dynamics. Hence, non-reversibility helps with the acceleration in the context of constrained sampling.
- Finally, we provide numerical experiments to show the efficiency of our proposed algorithm. Our numerical experiments are conducted using both synthetic data and real data. In particular, we start with a toy example of sampling the truncated standard multivariate normal distribution. Then, we conduct constrained Bayesian linear regression and constrained Bayesian logistic regression using synthetic data. Finally, we apply constrained Bayesian logistic regression to real datasets. Our numerical results indicate that by appropriately choosing the anti-symmetric matrix and the skew-projection, the proposed algorithm can outperform the PLMC algorithm in the existing literature.

Comparing with the literature on constrained sampling using Langevin algorithms, [BEL15, BEL18, Lam21] are the most relevant to our paper. When anti-symmetric matrix  $J(\cdot) \equiv 0$ , our

algorithm SRNLMC covers PLMC as a special case. Even though our model is more general, our technical assumptions are weaker. Instead of assuming that the target function is log-concave or strongly log-concave as in [BEL15, BEL18, Lam21], we relax this requirement by only imposing the existence of a spectral gap. The precise conditions for this are detailed in Assumption 2.10, followed by detailed discussions afterwards.

The paper is organized as follows. We state the main results in Section 2. In particular, we show the existence of the Skorokhod problem in Section 2.1. In Section 2.2, we study the continuous-time dynamics, and show that the Gibbs distribution is an invariant distribution, and provide non-asymptotic convergence result in TV and 1-Wasserstein distances. We provide discretization analysis in Section 2.3 by obtaining discretization error in 1-Wasserstein distance, and as a consequence, the iteration complexity of the discrete-time algorithm. Finally, numerical experiments are provided in Section 3.

## 2 Main Results

Throughout this work, we make the following assumptions for the domain  $\mathcal{C}$ , the target function  $f$ , and the skew function  $J$ :

**Assumption 2.1** (Domain Assumption). The domain  $\mathcal{C}$  is bounded, convex, and has a  $C^1$  boundary  $\partial\mathcal{C}$ . For the convenience of the analysis, we further assume that  $0 \in \mathcal{C}$  and  $\mathcal{C}$  is contained in a ball centered at 0 with radius  $R > 0$  and contains a ball centered at 0 with radius  $r > 0$ .

**Assumption 2.2** (Lipschitz Conditions). The gradient of the target function  $\nabla f$  and the operator  $J$  satisfy the Lipschitz condition, i.e., there exist constants  $L, L_J > 0$  such that:

$$\|\nabla f(x) - \nabla f(y)\| \leq L\|x - y\| \quad \text{and} \quad \|J(x) - J(y)\| \leq L_J\|x - y\|,$$

for all  $x, y \in \mathcal{C}$ .

Note that Assumption 2.1 and Assumption 2.2 imply that for any  $x \in \mathcal{C}$ ,  $\|J(x)\| \leq \|J(0)\| + L_J\|x\| \leq \|J\|_\infty := \|J(0)\| + L_J R$ . Similarly, for any  $x \in \mathcal{C}$ ,  $\|\nabla f(x)\| \leq \|\nabla f\|_\infty := \|\nabla f(0)\| + LR$ . This implies that  $J\nabla f$  is  $(\|J\|_\infty L + \|\nabla f\|_\infty L_J)$ -Lipschitz.

### 2.1 Skorokhod Problem

In this section, we first show the existence of the Skorokhod problem with skew-unit inner normal vector corresponding to (1.5).

**Lemma 2.3.** *For a non-reversible Langevin SDE takes the form of (1.4), there exists a skew-reflected non-reversible Langevin dynamics in the form of (1.5), and the solution is unique in the strong sense.*

*Proof.* The proof follows from solving the Skorokhod problem for the non-reversible Langevin SDE (1.4). The existence of the solution for the Skorokhod problem follows from [Tan79][Theorem 4.2], see also [LS84]. In the current setting, our reflection is defined through a skew-unit vector  $\nu^J$  in (1.6). To be precise, the discretization of the non-reversible SDE is kept inside the domain by skew-projection (1.9):

$$x_{k+1} = \mathcal{P}_C^J \left( x_k - \eta(I + J(x_k))\nabla f(x_k) + \sqrt{2\eta}\xi_k \right).$$

The inner unit normal vector associated with the standard projection map  $\mathcal{P}_C$  is defined as, for  $s = k\eta$ :

$$\nu_s = -\frac{\tilde{x}_{k+1} - \mathcal{P}_C(\tilde{x}_{k+1})}{\|\tilde{x}_{k+1} - \mathcal{P}_C(\tilde{x}_{k+1})\|}.$$

where

$$\tilde{x}_{k+1} := x_k - \eta(I + J(x_k))\nabla f(x_k) + \sqrt{2\eta}\xi_{k+1}. \quad (2.1)$$

We then define the inner skew-unit normal vector  $\nu_s^J$  sharing the same origin on the boundary with  $\nu_s$  as below:

$$\nu_s^J := \frac{\mathcal{R}_C^J(\tilde{x}_{k+1}) - \mathcal{P}_C(\tilde{x}_{k+1})}{\|\mathcal{R}_C^J(\tilde{x}_{k+1}) - \mathcal{P}_C(\tilde{x}_{k+1})\|},$$

where  $\tilde{x}_{k+1}$  is defined in (2.1). Following from our definition, we observe that

$$\nu^J(X_s) = \frac{(I + J(X_s))\nu_s}{\sqrt{\|\nu_s\|^2 + \|J\nu_s\|^2}},$$

which ensures that  $\mathcal{P}_C^J$  keeps the trajectory inside the domain  $\mathcal{C}$ . Since  $x_k - \eta(I + J(x_k))\nabla f(x_k)$  are constant on each of the time interval  $[k\eta, (k+1)\eta)$ , we are thus reduced to solve a Skorokhod problem with skew-reflection on the boundary. In particular, the existence of solution for the SDE with skew-reflection following from [Tan79][Remark 2.1]. The unit vector  $\nu_s^J$  does not need to be normal, but satisfying  $\langle \nu_t^J - X_t, L(dt) \rangle \geq 0$ , which is true following from our definition of  $\nu^J$ . We thus show the existence of the solution. Under Assumption 2.2, and following the results in [DI93], which establish the properties of SDEs with oblique reflection in non-smooth domains, we deduce the uniqueness of the strong solution.  $\square$

## 2.2 Continuous-time analysis

Our first main result is that the Gibbs distribution constrained on  $\mathcal{C}$  is an invariant measure for the  $X_t$  process in (1.5). Before we proceed, we derive the infinitesimal generator for  $X_t$  process in (1.5).

**Lemma 2.4.** *The infinitesimal generator  $\mathcal{L}$  for  $X_t$  process in (1.5) is given as follows. For any  $g \in \mathcal{D}(\mathcal{L})$ :*

$$\mathcal{L}g := -\langle \nabla g, (I + J)\nabla f \rangle + \Delta g, \quad (2.2)$$

subject to the Neumann boundary condition:

$$\nabla g \cdot \nu^J = 0. \quad (2.3)$$

**Remark 2.5.** Notice that, the Neumann boundary condition (2.3) is equivalent to the following condition,

$$\nabla g(x) \cdot \nu(x) = (J(x)\nabla g(x)) \cdot \nu(x), \quad \text{for any } x \in \partial\mathcal{C}. \quad (2.4)$$

*Proof of Lemma 2.4.* Let us prove that the infinitesimal generator for  $X_t$  process in (1.5) is given by  $\mathcal{L}$  (2.2) with the boundary condition (2.3). Let  $P_t$  be the semigroup associated with  $X_t$ , where  $X_t$  satisfies (1.5). In other words, for given  $g \in \mathcal{D}(\mathcal{L})$ ,

$$P_t g(x) := \mathbb{E}^x [g(X_t)] = \mathbb{E} [g(X_t) | X_0 = x].$$

By Itô's formula, we have that

$$\begin{aligned} g(X_t) - g(x) &= \int_0^t \langle \nabla g(X_s), -(I + J(X_s))\nabla f(X_s) \rangle ds + \int_0^t \sqrt{2} \langle \nabla g(X_s), dW_s \rangle \\ &\quad + \int_0^t \Delta g(X_s) ds + \int_0^t \langle \nabla g(X_s), \nu^J(X_s) \rangle L(ds), \end{aligned} \quad (2.5)$$

where the second term on the right hand side of (2.5) is a martingale and the last term in (2.5) vanishes by the boundary condition for  $g$  (see (2.3)). Then we get that

$$\mathcal{L}g := \lim_{t \downarrow 0} \frac{P_t g - g}{t} = \lim_{t \downarrow 0} \frac{\mathbb{E}^x [g(X_t)] - g(x)}{t} = -\langle -\nabla g, (I + J)\nabla f \rangle + \Delta g,$$

which verifies (2.2). □

Now, we are ready to state our first main result.

**Theorem 2.6.** *The Gibbs distribution  $\pi \propto e^{-f(x)}$ ,  $x \in \mathcal{C}$  is an invariant measure for the  $X_t$  process in (1.5).*

*Proof.* First, we can write

$$d\pi(x) = \frac{1}{Z} e^{-f(x)} dx, \quad x \in \mathcal{C}, \quad (2.6)$$

where

$$Z = \int_{\mathcal{C}} e^{-f(x)} dx \quad (2.7)$$

is the normalizing constant.

Next, we recall that the  $X_t$  process in (1.5) has the infinitesimal generator  $\mathcal{L}$  as given in (2.2). For any  $g \in \mathcal{D}(\mathcal{L})$ , we can compute that

$$\int_{\mathcal{C}} \mathcal{L}g(x) d\pi(x)$$

$$\begin{aligned}
&= - \int_{\mathcal{C}} \langle \nabla g(x), (I + J(x)) \nabla f(x) \rangle d\pi(x) + \int_{\mathcal{C}} \Delta g(x) d\pi(x) \\
&= \frac{1}{Z} \left( - \int_{\mathcal{C}} \langle \nabla g(x), (I + J(x)) \nabla f(x) \rangle e^{-f(x)} dx + \int_{\mathcal{C}} \Delta g(x) e^{-f(x)} dx \right) \\
&= \frac{1}{Z} \left( - \int_{\mathcal{C}} \langle (I + J^\top(x)) \nabla g(x), \nabla f(x) \rangle e^{-f(x)} dx + \int_{\mathcal{C}} \langle \nabla, (I + J^\top(x)) \nabla g(x) \rangle e^{-f(x)} dx \right) \\
&= \frac{1}{Z} \int_{\mathcal{C}} \nabla \cdot \left( (I + J^\top(x)) \nabla g(x) e^{-f(x)} \right) dx \\
&= 0, \tag{2.8}
\end{aligned}$$

where we used the boundary condition (2.3), and the fact  $\langle a, Mb \rangle = \langle M^\top a, b \rangle$  for any matrix  $M \in \mathbb{R}^{d \times d}$  and vectors  $a, b \in \mathbb{R}^d$  and the fact that  $J$  is an anti-symmetric matrix such that  $J^\top = -J$  and thus  $\langle \nabla, J^\top \nabla g \rangle = 0$ . Hence,  $\pi \propto e^{-f(x)}$ ,  $x \in \mathcal{C}$  is an invariant measure for the  $X_t$  process in (1.5).  $\square$

Indeed, we can establish the following commutator identity, which we will see later that it is a stronger result than Theorem 2.6 which implies Theorem 2.6.

**Lemma 2.7** (Commutator Identity). *Given  $g, h \in \mathcal{D}(\mathcal{L})$ , it holds that*

$$\int_{\mathcal{C}} h \mathcal{L} g d\pi - \int_{\mathcal{C}} g \mathcal{L} h d\pi = \int_{\mathcal{C}} \nabla \cdot (h J \nabla g - g J \nabla h) d\pi. \tag{2.9}$$

*Proof.*

$$\begin{aligned}
\int_{\mathcal{C}} h \mathcal{L} g d\pi &= \frac{1}{Z} \int_{\mathcal{C}} h \mathcal{L} g e^{-f} dx \\
&= \frac{1}{Z} \int_{\mathcal{C}} h (-\langle \nabla g, (I + J) \nabla f \rangle + \Delta g) e^{-f} dx \\
&= \frac{1}{Z} \int_{\mathcal{C}} h (-\langle (I - J) \nabla g, \nabla f \rangle + \Delta g) e^{-f} dx \\
&= \frac{1}{Z} \int_{\mathcal{C}} h \langle (I - J) \nabla g, \nabla e^{-f} \rangle + (h \Delta g) e^{-f} dx \\
&= -\frac{1}{Z} \int_{\mathcal{C}} \langle \nabla h, \nabla g \rangle e^{-f} dx + \frac{1}{Z} \int_{\mathcal{C}} \nabla \cdot (h J \nabla g) e^{-f} dx \\
&= - \int_{\mathcal{C}} \langle \nabla h, \nabla g \rangle d\pi + \int_{\mathcal{C}} \nabla \cdot (h J \nabla g) d\pi,
\end{aligned}$$

where  $Z > 0$  is the normalizing constant given in (2.7).

By swapping  $h$  and  $g$ , we get the identity (2.9).  $\square$



**Remark 2.8.** Lemma 2.7 is an extension of Theorem 2.6 in the sense that it implies Theorem 2.6. To see this, since  $\nabla \cdot J = 0$ , by letting  $h \equiv 1$ , we get that

$$\begin{aligned}
\int_{\mathcal{C}} \mathcal{L}g d\pi &= \int_{\mathcal{C}} \nabla \cdot (J \nabla g) d\pi \\
&= \int_{\mathcal{C}} \sum_{i=1}^d \sum_{j=1}^d \nabla_i (J_{ij} \nabla_j g) d\pi \\
&= \int_{\mathcal{C}} \sum_{i=1}^d \sum_{j=1}^d \nabla_i J_{ij} \nabla_j g d\pi + \int_{\mathcal{C}} \sum_{i=1}^d \sum_{j=1}^d J_{ij} \nabla_{ij} g d\pi \\
&= 0.
\end{aligned} \tag{2.10}$$

The first term in (2.10) is zero since  $\nabla \cdot J = 0$  and the second term in (2.10) is also zero because the anti-symmetry property of  $J$  and the symmetry of  $\nabla^2 g$ ; more precisely,

$$\sum_{i=1}^d \sum_{j=1}^d J_{ij} \nabla_{ij} g = \sum_{i=1}^d \sum_{j=1}^d J_{ij} \nabla_{ji} g = \sum_{i=1}^d \sum_{j=1}^d J_{ji} \nabla_{ij} g = - \sum_{i=1}^d \sum_{j=1}^d J_{ij} \nabla_{ij} g = 0.$$

**Remark 2.9.** Since  $\nabla \cdot J = 0$ , by letting  $h = g$ , we have the Dirichlet form:

$$\mathcal{E}(g, g) := \int_{\mathcal{C}} g \mathcal{L}g d\pi = - \int_{\mathcal{C}} \|\nabla g\|^2 d\pi. \tag{2.11}$$

Next, let us study the convergence speed of the continuous-time process  $X_t$  in (1.5) to its invariant distribution. Before we proceed, let us introduce two notions of non-asymptotic convergence bound here.

First, we let  $\lambda_J$  be the spectral gap of  $\mathcal{L}$  in  $L^2(\pi)$ , where the subscript emphasizes the dependence on the anti-symmetric matrix  $J$ . That is,

$$\int_{\mathcal{C}} (\mathbb{E}^x [g(X_t)] - \pi(g))^2 \pi(x) dx = \|P_t g - \pi(g)\|^2 \leq C_J \|g - \pi(g)\|^2 e^{-2\lambda_J t}, \tag{2.12}$$

for some constant  $C_J$ . In particular,  $\lambda_0$  denotes the spectral gap when  $J = 0$ , i.e. the case of the overdamped Langevin diffusion. We assume the existence of the spectral gap of  $\mathcal{L}$  when  $J = 0$ , i.e. it is positive.

**Assumption 2.10.** Assume that  $\lambda_0 > 0$ .

It is worth noting that the existence of a spectral gap can be derived from the logarithmic Sobolev inequality, as discussed in [BGL14]. Furthermore, the logarithmic Sobolev inequality itself can be established under the weaker condition of the existence of a Lyapunov function for the diffusion generator [BBCG08, CGW10]. Explicit lower bounds for the logarithmic Sobolev inequality in convex bounded domain have been explored in works such as [Wan97].

Next, we introduce the rate of convergence of  $p(t, x, y)$ , the transition probability density of  $X_t$ , to the Gibbs distribution  $\pi$  in the variational norm, which is equivalent to the TV distance up to a 1/2 factor. Let us define:

$$\rho_J := \sup \left\{ \rho : \int_{\mathcal{C}} |p(t, x, y) - \pi(y)| dy \leq g(x) e^{-\rho t} \right\}, \quad (2.13)$$

for some  $g(x)$  that may depend on  $J$ . In particular,  $\rho_0$  denotes the case when  $J = 0$ , i.e. the case of the overdamped Langevin diffusion.

We will obtain a non-asymptotic bound for the convergence of the distribution of  $X_t$  to the invariant distribution  $\pi$  in total variation (TV) distance and 1-Wasserstein distance.

**Theorem 2.11.** *There exists some constant  $\mathcal{K} > 0$  such that for any  $X_0 = x \in \mathcal{C}$ ,*

$$\text{TV}(\text{Law}(X_t), \pi) \leq \mathcal{K} e^{-\rho_J t}, \quad (2.14)$$

where  $\rho_J \geq \rho_0 > 0$ . In addition,

$$\mathcal{W}_1(\text{Law}(X_t), \pi) \leq 2R \cdot \mathcal{K} e^{-\rho_J t}, \quad (2.15)$$

Theorem 2.11 is inspired by the result for the convergence of (1.4) to the invariant distribution for the unconstrained domain in [HHMS05]. Since our  $\mathcal{C}$  is bounded, we are able to obtain a convergence bound in Theorem 2.11 uniformly in the initial starting point  $X_0 = x \in \mathcal{C}$ . Moreover, in addition to the TV distance, we also have the 1-Wasserstein guarantee in Theorem 2.11. To prove Theorem 2.11, we will establish a sequence of technical lemmas.

**Lemma 2.12.**  $\lambda_J \geq \lambda_0$ .

*Proof of Lemma 2.12.* We follow the similar argument as in the proof of Theorem 1 in [HHMS05] for the unconstrained case. If  $g \in \mathcal{D}(\mathcal{L})$ , then  $g \in \mathcal{D}(\mathcal{E})$  and

$$\mathcal{E}(g, g) \leq - \int_{\mathcal{C}} (\mathcal{L}g)g d\pi, \quad (2.16)$$

(see page 124 in [Sta99]), where  $\mathcal{E}(\cdot, \cdot)$  is the Dirichlet form in (2.11). Indeed, (2.16) holds in a more general setting [Sta99], and in our case, the inequality becomes the equality in (2.16) (see our Equation (2.11)). For any  $g$  with  $\|g\| = 1$  and  $\pi(g) = 0$ , let  $h(t) := \|P_t g\|^2$ . Then  $h(0) = 1$  and by (2.16), we have

$$h'(t) = 2 \int_{\mathcal{C}} (\mathcal{L}P_t g)(P_t g) d\pi \leq -2\mathcal{E}(P_t g, P_t g) \leq -2\lambda_0 h(t). \quad (2.17)$$

This implies that the operator norm  $\|P_t\|$  in the space  $\{g : g \in L^2(\pi), \pi(g) = 0\}$  is less than or equal to  $e^{-\lambda_0 t}$ . Hence,  $\lambda_J \geq \lambda_0$ . This completes the proof.  $\square$

Next, we show the following lemma.

**Lemma 2.13.** *There exists some constant  $\mathcal{K} > 0$  such that for any  $X_0 = x \in \mathcal{C}$ ,*

$$\text{TV}(\text{Law}(X_t), \pi) \leq \mathcal{K}e^{-\rho_J t}, \quad (2.18)$$

where  $\rho_J \geq \lambda_J$ .

*Proof of Lemma 2.13.* The proof is inspired by that of Theorem 4 in [HHMS05] for the unconstrained case. Let  $p_t(x, y) := p(t, x, y)/\pi(y)$  for any  $x, y \in \mathcal{C}$ , where  $p(t, x, y)$  denotes the probability density function for  $X_t$  given that  $X_0 = x \in \mathcal{C}$ . By the definition of the TV distance, we have

$$\text{TV}(\text{Law}(X_t), \pi) = \int_{\mathcal{C}} |p(t, x, y) - \pi(y)| dy = \int_{\mathcal{C}} |p_t(x, y) - 1| \pi(y) dy. \quad (2.19)$$

By letting  $p_t^*(\cdot, \cdot)$  denote the adjoint process, we can compute that for any  $t \geq 1$ ,

$$\begin{aligned} \int_{\mathcal{C}} |p_t(x, y) - 1| \pi(y) dy &= \int_{\mathcal{C}} \left| \int_{\mathcal{C}} (p_1(x, z) p_{t-1}(z, y) - 1) \pi(z) dz \right| \pi(y) dy \\ &= \int_{\mathcal{C}} \left| \int_{\mathcal{C}} (p_1(x, z) p_{t-1}^*(y, z) - 1) \pi(z) dz \right| \pi(y) dy \\ &= \int_{\mathcal{C}} \left| \int_{\mathcal{C}} p_{t-1}^*(y, z) p_1(x, z) \pi(z) dz - \int_{\mathcal{C}} p_1(x, z) \pi(z) dz \right| \pi(y) dy \\ &= \int_{\mathcal{C}} |P_{t-1}^*(p_1(x, \cdot))(y) - \pi(p_1(x, \cdot))| \pi(y) dy \\ &\leq \left( \int_{\mathcal{C}} |P_{t-1}^*(p_1(x, \cdot))(y) - \pi(p_1(x, \cdot))|^2 \pi(y) dy \right)^{1/2} \\ &\leq C \|p_1(x, \cdot) - 1\| e^{-\lambda_J t}, \end{aligned}$$

where we used Cauchy-Schwarz inequality and  $C$  is some constant. By applying the regularity estimates for oblique parabolic equations from [Lie90], we conclude that  $p_1(x, \cdot)$  is Hölder continuous on  $\mathcal{C}$ . Consequently,  $p_1(x, \cdot) \in L^2(\pi)$ , and thus, the final inequality holds. This also establishes that  $\rho_J \geq \lambda_J$ .  $\square$

Next, we show that  $\lambda_0 = \rho_0$ .

**Lemma 2.14.**  $\lambda_0 = \rho_0$ .

*Proof of Lemma 2.14.* The proof is inspired by that of Theorem 5 in [HHMS05] for the unconstrained case. When  $J = 0$ ,  $X_t$  is reversible and  $P_t$  is self-adjoint in  $L^2(\pi)$ . Given  $g$  with  $\pi(g) = 0$  and  $g \in C^\infty$ , we have

$$\|P_t g\|^2 = \pi(g P_{2t} g)$$

$$\begin{aligned}
&= \int_{\mathcal{C}} g(x) \left( \int_{\mathcal{C}} (p_{2t}(x, y) - 1) g(y) \pi(y) dy \right) \pi(x) dx \\
&\leq \sup_{x \in \mathcal{C}} \|g(x)\|^2 \int_{\mathcal{C}} \int_{\mathcal{C}} |p_{2t}(x, y) - 1| \pi(y) dy \pi(x) dx \\
&\leq \sup_{x \in \mathcal{C}} \|g(x)\|^2 \int_{\mathcal{C}} \mathcal{K} e^{-2\rho t} \pi(x) dx \\
&= \sup_{x \in \mathcal{C}} \|g(x)\|^2 \mathcal{K} e^{-2\rho t},
\end{aligned}$$

where we applied Lemma 2.13.

By Lemma 2.2. in [RW01], for  $s \leq t$  and  $\pi(g^2) = 1$ ,

$$\|P_s g\|^2 (\|P_t g\|^2)^{s/t} \leq \left( \sup_{x \in \mathcal{C}} \|g(x)\|^2 \mathcal{K} \right)^{s/t} e^{-2\rho_0 s}. \quad (2.20)$$

The equalities hold at  $s = 0$ . By taking derivative with respect to  $s$  and letting  $s = 0$ , we get

$$-2\mathcal{E}(g, g) \leq \frac{1}{t} \log \left( \sup_{x \in \mathcal{C}} \|g(x)\|^2 \mathcal{K} \right) - 2\rho_0, \quad (2.21)$$

where  $\mathcal{E}(g, g)$  is the Dirichlet form (2.11). By letting  $t \rightarrow \infty$ , we have

$$\mathcal{E}(g, g) \geq \rho_0. \quad (2.22)$$

This completes the proof.  $\square$

Now, we are finally ready to prove Theorem 2.11.

*Proof of Theorem 2.11.* It follows from Lemma 2.13 that there exists some constant  $\mathcal{K} > 0$  such that for any  $X_0 = x \in \mathcal{C}$ ,

$$\text{TV}(\text{Law}(X_t), \pi) \leq \mathcal{K} e^{-\rho_J t}, \quad (2.23)$$

where  $\rho_J \geq \lambda_J$ . We recall from Lemma 2.12 that  $\lambda_J \geq \lambda_0$  and from Lemma 2.14 that  $\lambda_0 = \rho_0$ . Hence, we conclude that  $\rho_J \geq \lambda_J \geq \lambda_0 = \rho_0 > 0$ , where we also used  $\lambda_0 > 0$  from Assumption 2.10. Finally, we have the inequality

$$\mathcal{W}_1(\text{Law}(X_t), \pi) \leq 2R \cdot \text{TV}(\text{Law}(X_t), \pi), \quad (2.24)$$

which is due to the fact 1-Wasserstein distance can be bounded by TV distance on a bounded domain [GS02]. The proof is complete.  $\square$

In Theorem 2.11, we do not have an explicit bound on  $\rho_J$ . In general, it seems hard to show what is the optimal choice of  $J$  and how much acceleration you can obtain by comparing  $\rho_J$  to  $\rho_0$ . In what follows, we give an example on how to select matrix  $J$  when  $f(x) = x^\top H x$  and  $J$  are constant matrix.

**Proposition 2.15.** For  $f(x) = x^\top Hx$ , and  $H, J$  being constant matrices, we have

$$\mathcal{W}_1(\text{Law}(X_t), \pi) \leq 2Re^{-\tilde{\lambda}t}, \quad (2.25)$$

where  $\tilde{\lambda} > 0$  denotes the smallest eigenvalue of matrix  $(I + J)H$ .

*Proof.* We use the synchronous coupling method to establish the proof. Consider another coupled process  $\tilde{X}_t$  being a copy of  $X_t$  as defined in (1.5), driven by the same Brownian motion, satisfying the following dynamic,

$$d\tilde{X}_t = -(I + J)\nabla f(\tilde{X}_t)dt + \sqrt{2}dB_t + \nu^J(\tilde{X}_t)\tilde{L}(dt). \quad (2.26)$$

Consider the difference equation for  $X_t - \tilde{X}_t$  defined by (1.5) and (2.26) with constant matrix  $J$  and  $f(x) = x^\top Hx$ , we have the following differential equation

$$\begin{aligned} d(X_t - \tilde{X}_t) &= -[(I + J)\nabla f(X_t) - (I + J)\nabla f(\tilde{X}_t)]dt + \nu^J(X_t)L(dt) - \nu^J(\tilde{X}_t)\tilde{L}(dt) \\ &= -(I + J)H(X_t - \tilde{X}_t)dt + \nu^J(X_t)L(dt) - \nu^J(\tilde{X}_t)\tilde{L}(dt). \end{aligned} \quad (2.27)$$

Applying (2.27) below, we get

$$\begin{aligned} d\|X_t - \tilde{X}_t\|^2 &= -2(X_t - \tilde{X}_t)^\top (I + J)H(X_t - \tilde{X}_t)dt \\ &\quad + (X_t - \tilde{X}_t)^\top \nu^J(X_t)L(dt) + (\tilde{X}_t - X_t)^\top \nu^J(\tilde{X}_t)\tilde{L}(dt) \\ &\leq -2(X_t - \tilde{X}_t)^\top (I + J)H(X_t - \tilde{X}_t)dt, \end{aligned} \quad (2.28)$$

where the last inequality follows from the fact  $(X_t - \tilde{X}_t)^\top \nu^J(X_t) = \langle X_t - \tilde{X}_t, \nu^J(X_t) \rangle \leq 0$ , for  $X_t \in \partial\mathcal{C}$ , since  $\nu^J$  is defined as the skew-inner unit vector at  $X_t$ , and  $X_t - \tilde{X}_t$  pointed outward. Similarly,  $(\tilde{X}_t - X_t)^\top \nu^J(\tilde{X}_t) \leq 0$ , for  $\tilde{X}_t \in \partial\mathcal{C}$ . Denote  $\tilde{\lambda} \geq 0$  as the smallest eigenvalue for matrix  $(I + J)H$ , we further get the following estimate,

$$\frac{d\|X_t - \tilde{X}_t\|^2}{dt} \leq -2\tilde{\lambda}\|X_t - \tilde{X}_t\|^2. \quad (2.29)$$

Apply the Gronwall's inequality, we conclude that

$$\|X_t - \tilde{X}_t\|^2 \leq e^{-2\tilde{\lambda}t}\|X_0 - \tilde{X}_0\|^2, \quad (2.30)$$

which further implies that

$$\|X_t - \tilde{X}_t\| \leq e^{-\tilde{\lambda}t}\|X_0 - \tilde{X}_0\|. \quad (2.31)$$

By letting  $\tilde{X}_0$  follow the invariant distribution  $\pi$ , and using that fact that  $\|X_0 - \tilde{X}_0\| \leq 2R$ , we conclude that

$$\mathcal{W}_1(\text{Law}(X_t), \pi) \leq 2Re^{-\tilde{\lambda}t}. \quad (2.32)$$

This completes the proof.  $\square$

The above proposition simplifies the problem to a matrix optimization problem such that the smallest eigenvalue of matrix  $(I + J)H$  is maximized for a given matrix  $H$  and the optimal matrix  $J$ . This is equivalent to minimize the maximum eigenvalue of matrix  $-(I + J)H$ . To be precise, denote  $\lambda_M(-(I + J)H)$  and  $\lambda_m(-(I + J)H)$  as the maximum and minimum eigenvalues of matrix  $-(I + J)H$  with all negative eigenvalues. Then, we have  $\tilde{\lambda} = -\lambda_M(-(I + J)H)$ . Following from [HHMS93b][Theorem 3.3], we have  $\lambda_m(-H) \leq \lambda_m(-(I + J)H) \leq \lambda_M(-(I + J)H) \leq \lambda_M(-H)$ , which guarantees the convergence improvement of the non-reversible dynamics since  $\tilde{\lambda} = -\lambda_M(-(I + J)H)$  as long as  $\langle H, JH \rangle = 0$ . The optimal choice of matrix  $J$  follows from minimizing the eigenvalue  $\lambda_M(-(I + J)H)$ , as detailed in [HHMS93b][Section 4]. Following [HHMS93b][Theorem 4.1] (see also [LNPI3b][Theorem 1]), we know that  $-\inf_J \lambda_M(-(I + J)H) = \text{trace}(H)/d$ . Thus,  $\sup_J \tilde{\lambda} = \text{trace}(H)/d$ . In practice, identifying the optimal  $J$  to achieve the optimal value  $-\inf_J \lambda_M(-(I + J)H)$  is challenging. An alternative approach is to perturb the non-reversible term  $J$  by introducing a scaled version  $\alpha J$ , where  $\alpha$  is a tuning parameter. While the eigenvalue  $\lambda_M(-(I + J)H)$  is not monotone in  $\alpha$ , this technique provides a feasible way to get a better convergence rate.

### 2.3 Discretization analysis

In this section, we quantify the discretization error between the discrete-time algorithm SRNLMC (1.10) and the continuous-time dynamics SRNLD (1.5). We will provide explicit discretization error bound in terms of 1-Wasserstein distance. Our discrete error analysis is inspired by that of PLMC [BEL15].

We recall from (1.5) that  $X_t$  is the continuous-time process satisfying

$$dX_t = -(I + J(X_t))\nabla f(X_t)dt + \sqrt{2}dW_t + \nu^J(X_t)L(dt), \quad (2.33)$$

and we let  $\bar{X}(t)$  denote the continuous-time interpolation of the discrete algorithm such that  $\bar{X}(k\eta)$  has the same distribution as  $x_k$  for every  $k$ , i.e.  $\bar{X}_t := X_{\eta\lfloor t/\eta \rfloor}$ .

**Lemma 2.16.**

$$\mathbb{E} \left[ \int_0^t h_{\mathcal{C}}(-\nu^J(X_s))L(ds) \right] \leq \frac{\|x\|^2}{2} + t(d + RL(1 + \|J\|_{\infty})), \quad (2.34)$$

where  $h_{\mathcal{C}}$  is the support function of  $\mathcal{C}$ , i.e.  $h_{\mathcal{C}}(y) := \sup\{\langle x, y \rangle : x \in \mathcal{C}\}$  for every  $y \in \mathbb{R}^d$ .

*Proof.* By Itô's formula, we can compute that

$$\begin{aligned} \|X_t\|^2 - \|X_0\|^2 &= 2 \int_0^t \langle X_s, -(I + J(X_s))\nabla f(X_s) \rangle ds + 2 \int_0^t \sqrt{2} \langle X_s, dW_s \rangle \\ &\quad + 2dt + 2 \int_0^t \langle X_s, \nu^J(X_s) \rangle L(ds), \end{aligned} \quad (2.35)$$

where  $X_0 = x$ . Note that for any  $t$  in the support of  $L$ ,

$$\langle X_t, -\nu^J(X_t) \rangle \geq h_{\mathcal{C}}(-\nu^J(X_t)), \quad (2.36)$$

since we know

$$\langle X_t, -\nu(X_t) \rangle \geq \langle x, -\nu(X_t) \rangle \geq h_{\mathcal{C}}(-\nu^J(X_t)), \quad (2.37)$$

for any  $x \in \mathcal{C}$ , and  $\langle \nu^J(X_t), \nu(X_t) \rangle \geq \delta_0 > 0$ . This implies that

$$\begin{aligned} \mathbb{E} \left[ \int_0^t h_{\mathcal{C}}(-\nu^J(X_s)) L(ds) \right] &\leq \mathbb{E} \left[ - \int_0^t \langle X_s, \nu^J(X_s) \rangle L(ds) \right] \\ &= dt + \frac{\|x\|^2 - \mathbb{E}\|X_t\|^2}{2} + \mathbb{E} \left[ \int_0^t \langle X_s, -(I + J(X_s)) \nabla f(X_s) \rangle ds \right] \\ &\leq \frac{\|x\|^2}{2} + t(d + RL(1 + \|J\|_{\infty})). \end{aligned} \quad (2.38)$$

This completes the proof.  $\square$

Let  $\|\cdot\|_{\mathcal{C}}$  be the gauge of  $\mathcal{C}$ , that is,

$$\|x\|_{\mathcal{C}} = \inf\{t \geq 0 : x \in t\mathcal{C}\}, \quad \text{for any } x \in \mathcal{C}. \quad (2.39)$$

Next, we let

$$Z_t = \sqrt{2}W_t - \int_0^t (I + J(X_s)) \nabla f(X_s) ds, \quad (2.40)$$

and  $\bar{Z}_t := Z_{\eta\lfloor t/\eta \rfloor}$  be the continuous interpolation of the discretization of  $Z_t$ . We have the following technical lemma.

**Lemma 2.17.** *There exists a universal constant  $C > 0$  such that*

$$\mathbb{E} \left[ \sup_{s \in [0, t]} \|Z_s - \bar{Z}_s\|_{\mathcal{C}} \right] \leq CM_{\mathcal{C}} \sqrt{2d\eta} \sqrt{\log(t/\eta)} + \frac{\eta(1 + \|J\|_{\infty})L}{r}, \quad (2.41)$$

where  $M_{\mathcal{C}} := \mathbb{E}[\|U\|_{\mathcal{C}}]$ , where  $U$  is uniformly distributed on the sphere  $\mathbb{S}^{d-1}$ .

*Proof.* First of all, for any  $x \in \mathcal{C}$ , by Assumption 2.1 and Assumption 2.2, we have

$$\|(I + J(x)) \nabla f(x)\|_{\mathcal{C}} \leq \frac{1}{r} \|(I + J(x)) \nabla f(x)\| \leq \frac{(1 + \|J\|_{\infty})L}{r}. \quad (2.42)$$

Therefore, for any  $t > 0$ ,

$$\|Z_t - \bar{Z}_t\|_{\mathcal{C}} \leq \sqrt{2}\|W_t - \bar{W}_t\|_{\mathcal{C}} + \int_{\eta\lfloor t/\eta \rfloor}^t \|(I + J(X_s)) \nabla f(X_s)\|_{\mathcal{C}} ds$$

$$\leq \sqrt{2}\|W_t - \bar{W}_t\|_{\mathcal{C}} + \frac{\eta(1 + \|J\|_{\infty})L}{r}, \quad (2.43)$$

where  $\bar{W}_t := W_{\eta\lfloor t/\eta\rfloor}$  be the continuous interpolation of the discretization of the Brownian motion  $W_t$ . It follows from Lemma 3 in [BEL15] that there exists a universal constant  $C > 0$  such that

$$\mathbb{E} \left[ \sup_{s \in [0, t]} \|W_s - \bar{W}_s\|_{\mathcal{C}} \right] \leq CM_C \sqrt{d\eta} \sqrt{\log(t/\eta)}. \quad (2.44)$$

This completes the proof.  $\square$

**Lemma 2.18.** For any  $T \geq 0$ ,

$$\begin{aligned} \mathbb{E}\|X_T - \bar{X}_T\| &\leq \sqrt{2} \left( \sqrt{C} \sqrt{M_C} (2d\eta)^{1/4} (\log(T/\eta))^{1/4} + \frac{\eta(1 + \|J\|_{\infty})L}{r} \right) \\ &\quad \cdot \left( \frac{R}{\sqrt{2}} + \sqrt{T} (d + RL(1 + \|J\|_{\infty}))^{1/2} \right), \end{aligned} \quad (2.45)$$

where  $C > 0$  is a universal constant.

*Proof.* For any  $T \geq 0$ , by following the similar argument as in the proof of Proposition 1 in [BEL15], we have

$$\|X_T - \bar{X}_T\|^2 \leq 2 \int_0^T \langle Z_t - \bar{Z}_t, -\nu^J(X_t) \rangle L(dt). \quad (2.46)$$

Since  $\langle x, y \rangle \leq \|x\|_{\mathcal{C}} h_{\mathcal{C}}(y)$ , we have

$$\|X_T - \bar{X}_T\|^2 \leq 2 \sup_{t \in [0, T]} \|Z_t - \bar{Z}_t\|_{\mathcal{C}} \int_0^T h_{\mathcal{C}}(-\nu^J(X_t)) L(dt). \quad (2.47)$$

By Cauchy-Schwarz inequality and applying Lemma 2.16 and Lemma 2.17, we get

$$\begin{aligned} \mathbb{E}\|X_T - \bar{X}_T\| &\leq \sqrt{2} \left( \mathbb{E} \left[ \sup_{t \in [0, T]} \|Z_t - \bar{Z}_t\|_{\mathcal{C}} \right] \right)^{1/2} \left( \mathbb{E} \left[ \int_0^T h_{\mathcal{C}}(-\nu^J(X_t)) L(dt) \right] \right)^{1/2} \\ &\leq \sqrt{2} \left( CM_C \sqrt{2d\eta} \sqrt{\log(T/\eta)} + \frac{\eta(1 + \|J\|_{\infty})L}{r} \right)^{1/2} \\ &\quad \cdot \left( \frac{\|x\|^2}{2} + T (d + RL(1 + \|J\|_{\infty})) \right)^{1/2} \\ &\leq \sqrt{2} \left( \sqrt{C} \sqrt{M_C} (2d\eta)^{1/4} (\log(T/\eta))^{1/4} + \frac{\eta(1 + \|J\|_{\infty})L}{r} \right) \\ &\quad \cdot \left( \frac{R}{\sqrt{2}} + \sqrt{T} (d + RL(1 + \|J\|_{\infty}))^{1/2} \right), \end{aligned} \quad (2.48)$$

where we used the inequality that  $\sqrt{x+y} \leq \sqrt{x} + \sqrt{y}$  for any  $x, y \geq 0$  and for any  $x \in \mathcal{C}$ ,  $\|x\| \leq R$ . This completes the proof.  $\square$



We immediately obtain the following corollary that bounds the 1-Wasserstein distance between the distribution of the discrete-time algorithm SRNLMC (1.10) and that of the continuous-time dynamics SRNLD (1.5).

**Corollary 2.19.** *For any  $K \in \mathbb{N}$ ,*

$$\mathcal{W}_1(\text{Law}(X_{K\eta}), \text{Law}(x_k)) \leq \sqrt{2} \left( \sqrt{C} \sqrt{M_C} (2d\eta)^{1/4} (\log(K))^{1/4} + \frac{\eta(1 + \|J\|_\infty)L}{r} \right) \cdot \left( \frac{R}{\sqrt{2}} + \sqrt{K\eta} (d + RL(1 + \|J\|_\infty))^{1/2} \right), \quad (2.49)$$

where  $C > 0$  is a universal constant.

*Proof.* This is a direct consequence of Lemma 2.18 and the definition of 1-Wasserstein distance.  $\square$

By combining Theorem 2.11 and Corollary 2.19, we obtain the non-asymptotic convergence guarantees for discrete-time algorithm SRNLMC to the target distribution in 1-Wasserstein distance.

**Theorem 2.20.** *For any  $K \in \mathbb{N}$ ,*

$$\mathcal{W}_1(\text{Law}(x_k), \pi) \leq 2RK e^{-\rho_J K \eta} + \sqrt{2} \left( \sqrt{C} \sqrt{M_C} (2d\eta)^{1/4} (\log(K))^{1/4} + \frac{\eta(1 + \|J\|_\infty)L}{r} \right) \cdot \left( \frac{R}{\sqrt{2}} + \sqrt{K\eta} (d + RL(1 + \|J\|_\infty))^{1/2} \right), \quad (2.50)$$

where  $C > 0$  is a universal constant.

*Proof.* It is a direct consequence of the triangle inequality

$$\mathcal{W}_1(\text{Law}(x_k), \pi) \leq \mathcal{W}_1(\text{Law}(x_k), \text{Law}(X_{k\eta})) + \mathcal{W}_1(\text{Law}(X_{k\eta}), \pi), \quad (2.51)$$

and by applying Theorem 2.11 and Corollary 2.19.  $\square$

Based on Theorem 2.20, we obtain the iteration complexity in terms of the accuracy level  $\varepsilon$ , the dimension  $d$  and the spectral gap  $\rho_J$  in the following corollary.

**Corollary 2.21.** *For any given accuracy level  $\varepsilon > 0$ ,  $\mathcal{W}_1(\text{Law}(x_k), \pi) \leq \tilde{\mathcal{O}}(\varepsilon)$  provided that*

$$K\eta = \frac{\log(1/\varepsilon)}{\rho_J}, \quad (2.52)$$

and

$$\eta \leq \frac{\rho_J^8 \varepsilon^4}{\log(1/\rho_J) d^5 \log(d) \log(1/\varepsilon)}, \quad (2.53)$$

where  $\tilde{\mathcal{O}}$  hides the dependence on  $\log \log(1/\varepsilon)$ ,  $\log \log(d)$  and  $\log \log(1/\rho_J)$ .

*Proof.* It follows from Theorem 2.20 that

$$\mathcal{W}_1(\text{Law}(x_k), \pi) \leq \mathcal{O}(e^{-\rho_J K \eta}) + \mathcal{O}\left((d\eta)^{1/4}(\log(K))^{1/4}(K\eta)^{1/2}d\right). \quad (2.54)$$

Therefore, for any given accuracy level  $\varepsilon > 0$ ,  $\mathcal{O}(e^{-\rho_J K \eta}) \leq \mathcal{O}(\varepsilon)$  provided that

$$K\eta = \frac{\log(1/\varepsilon)}{\rho_J}, \quad (2.55)$$

and

$$\begin{aligned} \mathcal{O}\left((d\eta)^{1/4}(\log(K))^{1/4}(K\eta)^{1/2}d\right) &\leq \mathcal{O}\left(d^{5/4}\eta^{1/4}\frac{(\log(1/\varepsilon))^2}{\rho_J^2}\left(\log\left(\frac{\log(1/\varepsilon)}{\eta\rho_J}\right)\right)^{1/4}\right) \\ &\leq \tilde{\mathcal{O}}(\varepsilon) \end{aligned} \quad (2.56)$$

given that

$$\eta \leq \frac{\rho_J^8 \varepsilon^4}{\log(1/\rho_J)d^5 \log(d) \log(1/\varepsilon)}, \quad (2.57)$$

where  $\tilde{\mathcal{O}}$  hides the dependence on  $\log \log(1/\varepsilon)$ ,  $\log \log(d)$  and  $\log \log(1/\rho_J)$ .  $\square$

**Remark 2.22.** Corollary 2.21 implies that for any given accuracy level  $\varepsilon > 0$ ,  $\mathcal{W}_1(\text{Law}(x_k), \pi) \leq \tilde{\mathcal{O}}(\varepsilon)$  by taking

$$\eta = \frac{\rho_J^8 \varepsilon^4}{\log(1/\rho_J)d^5 \log(d) \log(1/\varepsilon)}, \quad (2.58)$$

and

$$K = \frac{\log(1/\varepsilon)}{\eta\rho_J} = \frac{\log(1/\rho_J)d^5 \log(d) (\log(1/\varepsilon))^2}{\rho_J^9 \varepsilon^4} = \tilde{\mathcal{O}}\left(\frac{\log(1/\rho_J)d^5}{\rho_J^9 \varepsilon^4}\right), \quad (2.59)$$

which provides the iteration complexity of the algorithm, where  $\mathcal{O}$  hides the logarithmic dependence on  $d$ ,  $\varepsilon$ . Since  $\rho_J \geq \rho_0 > 0$  (see Theorem 2.11), SRNLMC achieves a lower complexity compared to PLMC ( $J = 0$ ) for the given accuracy level  $\varepsilon$ , and hence we showed the by breaking reversibility, in the context of constrained sampling, acceleration is achievable.

### 3 Numerical Experiments

In Section 3.1, we will first compare the *iteration complexity* of skew-reflected non-reversible Langevin Monte Carlo (SRNLMC) to the one of projected Langevin Monte Carlo (PLMC) in 1-Wasserstein distance by using synthetic data in a toy example of truncated standard multivariate normal distribution.

By introducing *stochastic gradients*, we will propose *skew-reflected non-reversible stochastic gradient Langevin dynamics* (SRNSGLD) and *projected stochastic gradient Langevin dynamics*

(PSGLD). In Section 3.2, we will compare SRNSGLD to PSGLD in terms of *mean squared error* by using synthetic data in the example of constrained Bayesian linear regression. Furthermore, we will consider the example of constrained Bayesian logistic regression and we compare the accuracy, which is defined as the ratio of the correctly predicted labels over the whole dataset in deep learning experiments, of the algorithms by using either synthetic or real data in Section 3.3.

### 3.1 Toy Example: Truncated Standard Multivariate Normal Distribution

Considering the truncated standard multivariate normal distribution in certain convex sets  $\mathcal{C} \in \mathbb{R}^3$  with density function:

$$f(x) = \frac{1}{(\sqrt{2\pi})^3} \exp\left\{-\frac{\|x\|^2}{2}\right\} \mathbf{1}_{\mathcal{C}}, \quad (3.1)$$

where  $\mathbf{1}_{\mathcal{C}}$  denotes the indicator function on  $\mathcal{C}$ . In our experiments, we take the convex constraint sets to be ball  $\mathcal{C}_1$  and cubic  $\mathcal{C}_2$  in  $\mathbb{R}^3$ :

$$\mathcal{C}_1 = \{x \in \mathbb{R}^3 : \|x\|_2^2 \leq 1\}, \quad \mathcal{C}_2 = [-1, 1]^3. \quad (3.2)$$

For these 2 choices of convex sets, we can derive their skew-projection formula explicitly by computing out the skew unit normal vector direction using geometry. We set the skewed matrix  $J = J_a$  in SRNLMC to be state-independent, that is defined as:

$$J_a = \begin{bmatrix} 0 & a & 0 \\ -a & 0 & a \\ 0 & -a & 0 \end{bmatrix}, \quad (3.3)$$

where  $a \neq 0$  is a self-chosen constant parameter. Then we approximate Gibbs distribution by the rejection sampling approach, i.e. sampling from the 3-dimensional standard normal distribution and discarding the sample points that are out of the constraint set until obtaining the required number of sample points. Finally, we compare the 1-Wasserstein distances to the approximate distribution of SRNLMC and PLMC in each dimension.

Let the constraint set be the ball  $\mathcal{C}_1$  defined in (3.2). We chose the skewed matrix  $J_1$  with  $a = 1$  in (3.3), and simulated  $n = 3000$  samples and took 5000 iterates starting from the initial point  $x_0 = [0.3, 0.6, -0.4]^\top$  with the stepsize  $\eta = 10^{-4}$ . In Figure 1, we showed the first 2 dimensions of the target distribution in the left panel, and the first 2 dimensions of the sample distributions by SRNLMC and PLMC in the middle and right panels. These results showed that both SRNLMC and PLMC can successfully converge to the truncated standard normal distribution in our setting. Then we compared the convergence of SRNLMC to PLMC by computing the 1-Wasserstein distance in each dimension. By taking 5000 iterations with the ball constraint  $\mathcal{C}_1$  defined in (3.2) for both PLMC and SRNLMC, we obtained the plots in Figure 2 where the blue line represents SRNLMC and the orange line represents PLMC in each subfigure. In the same line, we considered the constraint set to be the cubic  $\mathcal{C}_2$  defined in (3.2), and took  $J_2$  to be the

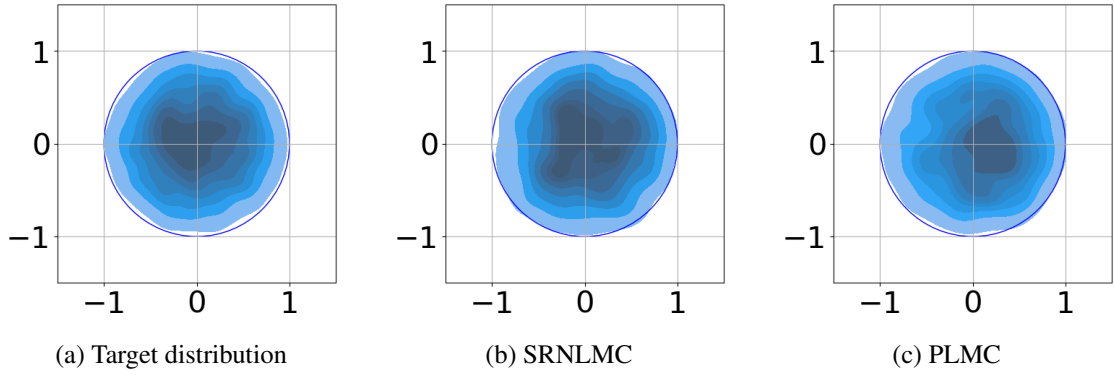


Figure 1: Visualized density plots for the first 2 dimensions in ball constraint

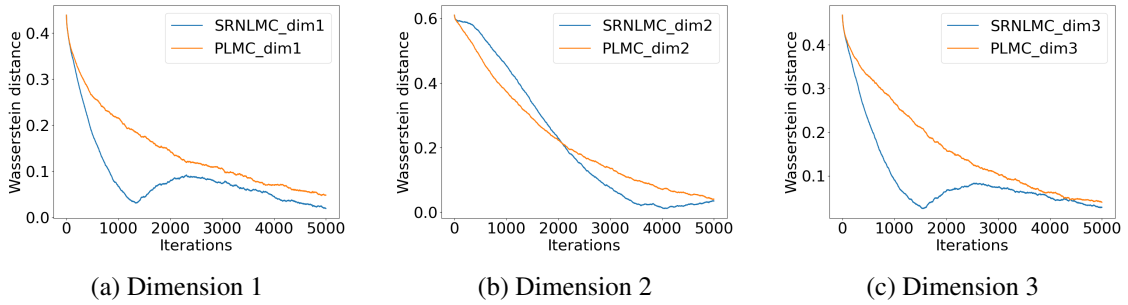


Figure 2: 1-Wasserstein distance in each dimension of PLMC and SRNLMC in ball constraint

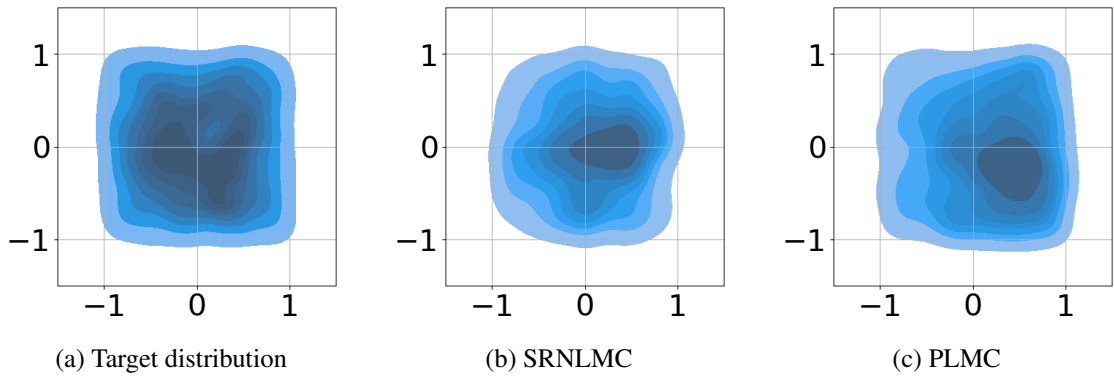


Figure 3: Visualized density plots for the first 2 dimensions in cubic constraint

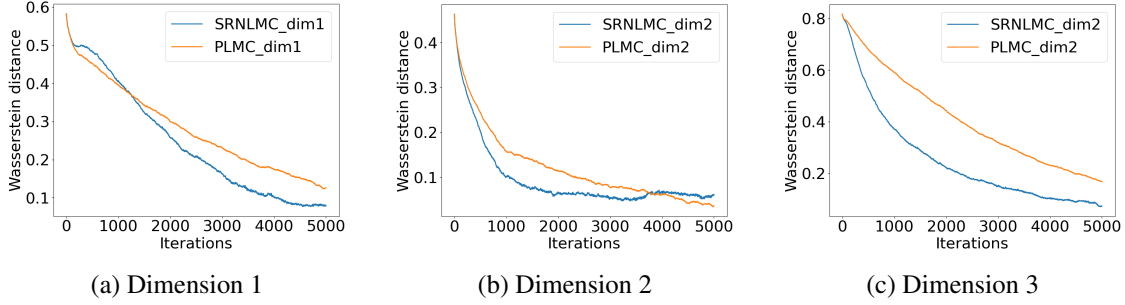


Figure 4: 1-Wasserstein distance in each dimension of PLMC and SRNLMLC in cubic constraint

skewed matrix with  $a = 2$  defined in (3.3), and the initial point to be  $x_0 = [0.5, -0.2, 0.8]^\top$ . The visualized results are shown in Figure 3 and the corresponding convergence results in Figure 4.

We can observe from Figure 2 and Figure 4 that with an appropriate chosen constant  $a \neq 0$  in skewed matrix  $J_a$  defined in (3.3), the iteration complexity of SRNLMLC is lower than the one of PLMC to achieve the same order of 1-Wasserstein distance between the sample and target distributions. This experiment result is consistent with our theoretical result in Theorem 2.20 that SRNLMLC can outperform PLMC, i.e. the skewed matrix  $J$  can help achieve acceleration in the constraint sampling problem.

### 3.2 Constrained Bayesian Linear Regression

In our next set of experiments, we test our algorithms in the constrained Bayesian linear regression models. In this experiment, we consider the case when the constraint set is a 2-dimensional centered unit disk such that

$$\mathcal{C} = \{x \in \mathbb{R}^2 : \|x\|_2^2 \leq 1\}, \quad (3.4)$$

which corresponds to the ridge Bayesian linear regression. We consider the linear regression model:

$$\delta_j \sim \mathcal{N}(0, 0.25), \quad a_j \sim \mathcal{N}(0, I), \quad y_j = x_\star^\top a_j + \delta_j, \quad x_\star = [1, 1]^\top. \quad (3.5)$$

The prior distribution is a uniform distribution, in which case the constraints are satisfied. Our goal is to generate the posterior distribution given by

$$\pi(x) \propto \exp \left\{ -\frac{1}{2} \sum_{j=1}^n (y_j - x^\top a_j)^2 \right\} \mathbf{1}_{\mathcal{C}}, \quad (3.6)$$

where  $\mathbf{1}_{\mathcal{C}}$  is the indicator function for the constraint set  $\mathcal{C}$  defined in (3.4) and  $n$  is the total number of data points in the training set.

For this experiment, to further illustrate the efficiency of our algorithms, we will introduce a stochastic gradient setting, and we will show that our algorithms work well in the presence of stochastic gradients.

In Section 1, we proposed *skew-reflected non-reversible Langevin Monte Carlo* (SRNLMC) algorithm (1.10). In practice, one often uses stochastic gradient, and we can therefore also consider the *skew-reflected non-reversible stochastic gradient Langevin dynamics* (SRNSGLD):

$$x_{k+1} = \mathcal{P}_{\mathcal{C}}^J \left( x_k - \eta(I + J(x_k))\nabla f(x_k, \Omega_{k+1}) + \sqrt{2\eta}\xi_{k+1} \right), \quad (3.7)$$

where  $\mathcal{P}_{\mathcal{C}}^J$  is the skew-projection onto  $\mathcal{C}$ ,  $\xi_k$  are i.i.d. Gaussian random vectors  $\mathcal{N}(0, I)$  and  $\nabla f(x_k, \Omega_{k+1})$  is a conditionally unbiased estimator of  $\nabla f(x_k)$ . For example, a common choice is the mini-batch setting, in which the full gradient is of the form  $\nabla f(x) = \frac{1}{n} \sum_{i=1}^n \nabla f_i(x)$ , where  $n$  is the number of data points and  $f_i(x)$  associates with the  $i$ -th data point, and the stochastic gradient is given by  $\nabla f(x_k, \Omega_{k+1}) := \frac{1}{b} \sum_{i \in \Omega_{k+1}} \nabla f_i(x_k)$  with  $b \ll n$  being the batch-size and  $\Omega_{k+1}^{(j)}$  are uniformly sampled random subsets of  $\{1, 2, \dots, n\}$  with  $|\Omega_{k+1}^{(j)}| = b$  and i.i.d. over  $k$ . If  $J \equiv 0$ , we obtain *projected stochastic gradient Langevin dynamics* (PSGLD).

Under the stochastic gradient setting, we chose the batch size  $b = 50$  and generated  $n = 10000$  data points  $(a_j, y_j)$  by SRNSGLD, where we took the skewed matrix  $J_2$  with  $a = 2$  defined by (3.3). By taking 600 iterations with the stepsize  $\eta = 10^{-4}$ , we get Figure 5 and Figure 6. In Figure 5, we present the prior uniform distribution in the left panel. In the middle and right panels, our simulation shows that both SRNSGLD and PSGLD can converge to the samples whose distribution concentrates around the closest position to the target value, with the red stars shown outside the constraints. In Figure 6, the blue line presents the mean squared error of SRNSGLD in 600 iterations and the that of PSGLD, where the mean squared error in the  $k$ -th run is computed by the formula  $\text{MSE}_k := \frac{1}{n} \sum_{j=1}^n \left( y_j - (x_k)^\top a_j \right)^2$ . Although we did not provide theoretical guarantees for the acceleration on the MSE, through our experiments, SRNSGLD demonstrates a better convergence performance.

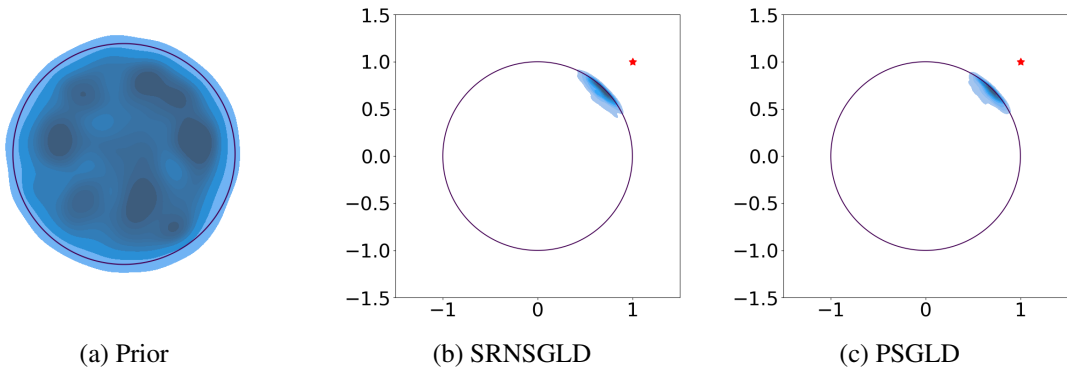


Figure 5: Prior and posterior distributions plot with disk constraint

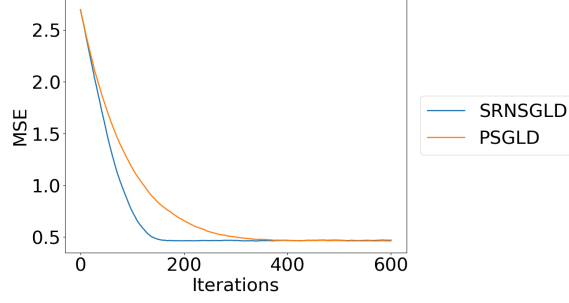


Figure 6: MSE result of SRNSGLD and PSGLD for the constrained Bayesian linear regression

### 3.3 Constrained Bayesian Logistic Regression

To test the performance of our algorithm in binary classification problems, we implement the constrained Bayesian linear regression models on both synthetic data and real data, where the constraint is the centered unit ball  $\mathcal{C}$  in  $\mathbb{R}^d$  such that

$$\mathcal{C} = \left\{ x \in \mathbb{R}^d : \|x\|_2^2 \leq 1 \right\}. \quad (3.8)$$

Suppose we can access a dataset  $Z = \{z_j\}_{j=1}^n$  where  $z_j = (X_j, y_j)$ ,  $X_j \in \mathbb{R}^d$  are the features and  $y_j \in \{0, 1\}$  are the labels with the assumption that  $X_j$  are independent and the probability distribution of  $y_j$  given  $X_j$  and the regression coefficients  $\beta \in \mathbb{R}^d$  are given by

$$\mathbb{P}(y_j = 1 \mid X_j, \beta) = \frac{1}{1 + e^{-\beta^\top X_j}}. \quad (3.9)$$

In all our experiments, we choose the prior distribution of  $\beta$  to be the uniform distribution in the ball constraint. Then the goal of the constrained Bayesian logistic regression is to sample from  $\pi(\beta) \propto e^{-f(\beta)} \mathbf{1}_{\mathcal{C}}$  with  $f(\beta)$ :

$$f(\beta) := - \sum_{j=1}^n \log p(y_j \mid X_j, \beta) - \log p(\beta) = \sum_{j=1}^n \log \left( 1 + e^{-\beta^\top X_j} \right) + \log V_d, \quad (3.10)$$

where  $V_d := \frac{\pi^{d/2}}{\Gamma(\frac{d}{2} + 1)}$  is the volume of the unit ball in  $\mathbb{R}^d$ .

#### 3.3.1 Synthetic data

Consider the following example of  $d = 3$ . First, we generated  $n = 2000$  synthetic data by the following model

$$X_j \sim \mathcal{N}(0, 2I_3), \quad p_j \sim \mathcal{U}(0, 1), \quad y_j = \begin{cases} 1 & \text{if } p_j \leq \frac{1}{1 + e^{-\beta^\top X_j}} \\ 0 & \text{otherwise} \end{cases}, \quad (3.11)$$

where  $\mathcal{U}(0, 1)$  is the uniform distribution on  $[0, 1]$  and the prior distribution of  $\beta = [\beta_1, \beta_2, \beta_3]^\top \in \mathbb{R}^3$  is a uniform distribution on the centered unit ball in  $\mathbb{R}^3$ . Then we implemented them with 1000 iterations by choosing the stepsize  $\eta = 10^{-4}$  and the batch size  $b = 50$ . For the constrained Bayesian logistic regression, it is not practical for us to compute the 1-Wasserstein distance between the approximated Gibbs distribution and the empirical distribution. Hence, for such a binary classification problem, we can use the accuracy over training set and test set to measure the goodness of the convergence performance.

In this experiment, we chose the skewed matrix  $J_2$  in (3.3) with  $a = 2$  for SRNSGLD and we used 20% of the whole dataset as the test set. The mean and standard deviation of the accuracy distribution are shown in Figure 7. We observe that to achieve the same level of accuracy among the test set, the SRNSGLD needs fewer iterations than the PSGLD.

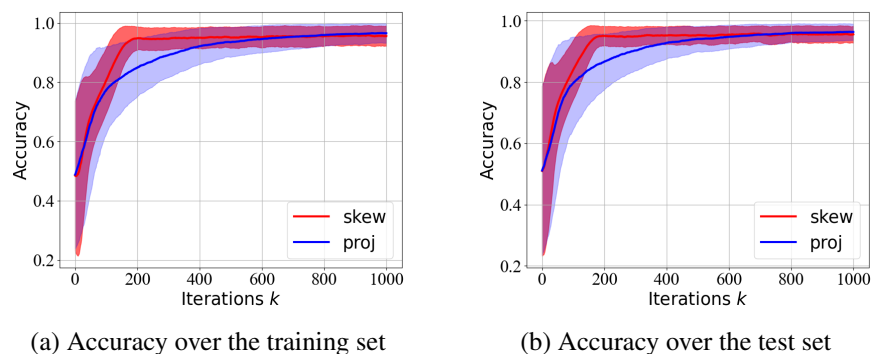


Figure 7: Accuracy over the training set and the test set for the synthetic data. The red part denotes the mean and standard deviation of SRNSGLD and the blue part denotes the mean and standard deviation of PSGLD.

### 3.3.2 Real data

In this section, we consider the constrained Bayesian logistic regression problem on the MAGIC Gamma Telescope dataset <sup>6</sup> and the Titanic dataset <sup>7</sup>. The Telescope dataset contains  $n = 19020$  samples with dimension  $d = 10$ , describing the registration of high energy gamma particles in a ground-based atmospheric Cherenkov gamma telescope using the imaging technique. The Titanic dataset contains 891 samples with 10 features representing information about the passengers. And the goal is to predict whether a passenger survived or not based on these features. However, some of the features are irrelevant to our goal, such as the ID number. Therefore, after a preprocessing on the raw dataset, we obtained a dataset containing  $n = 891$  labeled samples with  $d = 8$  features.

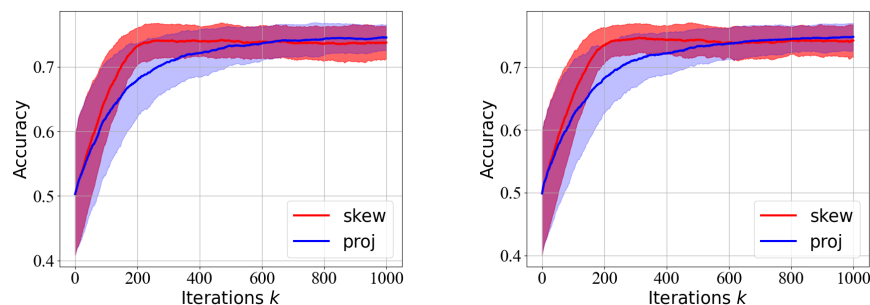
<sup>6</sup>The Telescope dataset is publicly available from:  
<https://archive.ics.uci.edu/ml/datasets/magic+gamma+telescope>.

<sup>7</sup>The Titanic dataset is publicly available from:  
<https://www.kaggle.com/c/titanic>.



For both of the datasets, we initialized the SRNSGLD and PSGLD with the uniform distribution on the centered unit ball in respective dimensions.

For the Telescope dataset, we set stepsize  $\eta = 10^{-4}$  and batch size  $b = 100$  and ran both SRNSGLD and PSGLD 1000 iterations over the training set, where we chose the skew matrix as  $J_{1.5}$  defined in (3.3) with  $a = 1.5$  for SRNSGLD. Figure 8 reports the accuracy of two algorithms over the training set and the test set where the test set counts for 20% of the whole dataset.

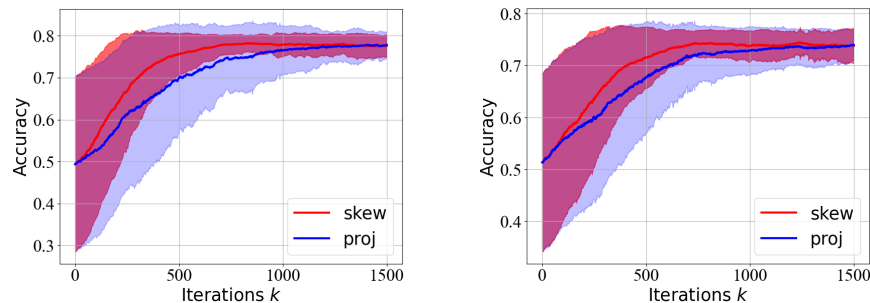


(a) Accuracy over the training set

(b) Accuracy over the test set

Figure 8: Accuracy over the training set and the test set for the telescope dataset. The red part denotes the mean and standard deviation of SRNSGLD and the blue part denotes the mean and standard deviation of PSGLD.

For the Titanic data, we set stepsize  $\eta = 10^{-4}$  and batch size  $b = 50$  and ran both SRNSGLD and PSGLD 1500 iterations over the training set, where we chose the skewed matrix  $J_2$  defined in (3.3) with  $a = 2$  for SRNSGLD. Figure 9 reported the accuracy level of two algorithms over the training and test sets where the test set counts for 20% of the whole dataset.



(a) Accuracy over the training set

(b) Accuracy over the test set

Figure 9: Accuracy over the training set and the test set for the Titanic dataset. The red part denotes the mean and standard deviation of SRNSGLD and the blue part denotes the mean and standard deviation of PSGLD.

We conclude from Figure 8 and Figure 9 that the highest accuracy SRNSGLD and PSGLD

can attained is in the similar level for both Telescope and Titanic datasets. However, The accuracy level of SRNSGLD improved at a faster rate than that of PSGLD. This experiment demonstrates that SRNSGLD is practically efficient.

## 4 Conclusion

In this paper, we studied the constrained sampling problem to sample from a target distribution on a constrained domain. We proposed and studied SRNLD, a continuous-time SDE with skew-reflected boundary. We obtained non-asymptotic convergence rate of SRNLD to the target distribution in both total variation and 1-Wasserstein distances. By breaking reversibility, we showed that the convergence rate is better than the special case of the reversible dynamics. We also proposed SRNLMC, based on the discretization of SRNLD, and obtained non-asymptotic discretization error from SRNLD, and provided convergence guarantees to the target distribution in 1-Wasserstein distance, that has better performance guarantees than PLMC based on the reversible dynamics in the literature. Hence, the acceleration is achievable by breaking reversibility in the context of constrained sampling. Numerical experiments are provided for both synthetic data and real data to show efficiency of the proposed algorithms.

## Acknowledgements

Qi Feng is partially supported by the grants NSF DMS-2306769 and DMS-2420029. Xiaoyu Wang is supported by the Guangzhou-HKUST(GZ) Joint Funding Program (No.2024A03J0630), Guangzhou Municipal Key Laboratory of Financial Technology Cutting-Edge Research. Lingjiong Zhu is partially supported by the grants NSF DMS-2053454 and DMS-2208303.

## References

- [AC21] Kwangjun Ahn and Sinho Chewi. Efficient constrained sampling via the mirror-Langevin algorithm. In *Advances in Neural Information Processing Systems (NeurIPS)*, volume 34, 2021.
- [ADFDJ03] Christophe Andrieu, Nando De Freitas, Arnaud Doucet, and Michael I Jordan. An introduction to MCMC for machine learning. *Machine Learning*, 50(1):5–43, 2003.
- [BBCG08] Dominique Bakry, Franck Barthe, Patrick Cattiaux, and Arnaud Guillin. A simple proof of the Poincaré inequality for a large class of probability measures. *Electronic Communications in Probability*, 13:60–66, 2008.
- [BEL15] Sebastien Bubeck, Ronen Eldan, and Joseph Lehec. Finite-time analysis of projected Langevin Monte Carlo. In *Advances in Neural Information Processing Systems*, volume 28, 2015.

- [BEL18] Sébastien Bubeck, Ronen Eldan, and Joseph Lehec. Sampling from a log-concave distribution with projected Langevin Monte Carlo. *Discrete & Computational Geometry*, 59(4):757–783, 2018.
- [BGL14] Dominique Bakry, Ivan Gentil, and Michel Ledoux. *Analysis and Geometry of Markov Diffusion Operators*, volume 103. Springer, 2014.
- [BGT04] Mireille Bossy, Emmanuel Gobet, and Denis Talay. A symmetrized Euler scheme for an efficient approximation of reflected diffusions. *Journal of Applied Probability*, 41(3):877–889, 2004.
- [CGW10] Patrick Cattiaux, Arnaud Guillin, and Li-Ming Wu. A note on Talagrand’s transportation inequality and logarithmic Sobolev inequality. *Probability Theory and Related Fields*, 148:285–304, 2010.
- [CLGL<sup>+</sup>20] Sinho Chewi, Thibaut Le Gouic, Cheng Lu, Tyler Maunu, Philippe Rigollet, and Austin Stromme. Exponential ergodicity of mirror-Langevin diffusions. In *Advances in Neural Information Processing Systems (NeurIPS)*, volume 33, 2020.
- [Cos92] Cristina Costantini. The Skorohod oblique reflection problem in domains with corners and application to stochastic differential equations. *Probability Theory and Related Fields*, 91:43–70, 1992.
- [DI93] Paul Dupuis and Hitoshi Ishii. SDEs with oblique reflection on nonsmooth domains. *Annals of Probability*, 21(1):554–580, 1993.
- [DLP16] Andrew B. Duncan, Tony Lelièvre, and Grigoris A. Pavliotis. Variance reduction using nonreversible Langevin samplers. *Journal of Statistical Physics*, 163(3):457–491, 2016.
- [DPZ17] Andrew B. Duncan, Grigoris A. Pavliotis, and Konstantinos C. Zygalakis. Nonreversible Langevin samplers: Splitting schemes, analysis and implementation. *arXiv preprint arXiv:1701.04247*, 2017.
- [FSS20] Futoshi Futami, Iseii Sato, and Masashi Sugiyama. Accelerating the diffusion-based ensemble sampling by non-reversible dynamics. In *Proceedings of the 37th International Conference on Machine Learning*, volume 119, pages 3337–3347. PMLR, 2020.
- [GCSR95] Andrew Gelman, John B Carlin, Hal S Stern, and Donald B Rubin. *Bayesian Data Analysis*. Chapman & Hall/CRC Press, 1995.
- [GGHZ21] Mert Gürbüzbalaban, Xuefeng Gao, Yunhan Hu, and Lingjiong Zhu. Decentralized stochastic gradient Langevin dynamics and Hamiltonian Monte Carlo. *Journal of Machine Learning Research*, 22(239):1–69, 2021.

- [GGZ20] Xuefeng Gao, Mert Gürbüzbalaban, and Lingjiong Zhu. Breaking reversibility accelerates Langevin dynamics for global non-convex optimization. In *Advances in Neural Information Processing Systems (NeurIPS)*, 2020.
- [GHZ24] Mert Gürbüzbalaban, Yuanhan Hu, and Lingjiong Zhu. Penalized overdamped and underdamped Langevin Monte Carlo algorithms for constrained sampling. *Journal of Machine Learning Research*, 25(263):1–67, 2024.
- [GIWZ24] Mert Gürbüzbalaban, Mohammad Rafiqul Islam, Xiaoyu Wang, and Lingjiong Zhu. Generalized EXTRA stochastic gradient Langevin dynamics. *arXiv preprint arXiv:2412.01993*, 2024.
- [GS02] Alison L. Gibbs and Francis Edward Su. On choosing and bounding probability metrics. *International Statistical Review*, 70(3):419–435, 2002.
- [HHMS93a] Chii-Ruey Hwang, Shu-Yin Hwang-Ma, and Shuenn-Jyi Sheu. Accelerating Gaussian diffusions. *Annals of Applied Probability*, 3:897–913, 1993.
- [HHMS93b] Chii-Ruey Hwang, Shu-Yin Hwang-Ma, and Shuenn-Jyi Sheu. Accelerating Gaussian Diffusions. *The Annals of Applied Probability*, 3(3):897 – 913, 1993.
- [HHMS05] Chii-Ruey Hwang, Shu-Yin Hwang-Ma, and Shuenn-Jyi Sheu. Accelerating diffusions. *Annals of Applied Probability*, 15:1433–1444, 2005.
- [HKRC18] Ya-Ping Hsieh, Ali Kavis, Paul Rolland, and Volkan Cevher. Mirrored Langevin dynamics. In *Advances in Neural Information Processing Systems*, volume 31, 2018.
- [HWG<sup>+</sup>20] Yuanhan Hu, Xiaoyu Wang, Xuefeng Gao, Gürbüzbalaban, and Lingjiong Zhu. Non-convex stochastic optimization via non-reversible stochastic gradient Langevin dynamics. *arXiv:2004.02823*, 2020. 45 pages.
- [Lam21] Andrew Lamperski. Projected stochastic gradient Langevin algorithms for constrained sampling and non-convex learning. In *Conference on Learning Theory*, volume 134, pages 2891–2937. PMLR, 2021.
- [Lie90] Gary A Lieberman. On the Hölder gradient estimate for solutions of nonlinear elliptic and parabolic oblique boundary value problems. *Communications in Partial Differential Equations*, 15(4):515–523, 1990.
- [LNP13a] Tony Lelièvre, Francis Nier, and Grigorios A Pavliotis. Optimal non-reversible linear drift for the convergence to equilibrium of a diffusion. *Journal of Statistical Physics*, 152(2):237–274, Jul 2013.
- [LNP13b] Tony Lelièvre, Francis Nier, and Grigorios A Pavliotis. Optimal non-reversible linear drift for the convergence to equilibrium of a diffusion. *Journal of Statistical Physics*, 152(2):237–274, 2013.

- [LS84] Pierre-Louis Lions and Alain-Sol Sznitman. Stochastic differential equations with reflecting boundary conditions. *Communications on Pure and Applied Mathematics*, 37(4):511–537, 1984.
- [LTVW22] Ruilin Li, Molei Tao, Santosh S. Vempala, and Andre Wibisono. The mirror Langevin algorithm converges with vanishing bias. In Sanjoy Dasgupta and Nika Haghtalab, editors, *Proceedings of The 33rd International Conference on Algorithmic Learning Theory*, volume 167, pages 718–742. PMLR, 2022.
- [RBS15a] Luc Rey-Bellet and Konstantinos Spiliopoulos. Irreversible Langevin samplers and variance reduction: a large deviation approach. *Nonlinearity*, 28:2081, 2015.
- [RBS15b] Luc Rey-Bellet and Konstantinos Spiliopoulos. Variance reduction for irreversible Langevin samplers and diffusion on graphs. *Electronic Communications in Probability*, 20(15):16 pp., 2015.
- [RBS16] Luc Rey-Bellet and Konstantinos Spiliopoulos. Improving the convergence of reversible samplers. *Journal of Statistical Physics*, 164(3):472–494, 2016.
- [RW01] Michael Röckner and Feng-Yu Wang. Weak Poincaré inequalities and  $L^2$ -convergence rates of Markov semigroups. *Journal of Functional Analysis*, 185:546–603, 2001.
- [SR20] Adil Salim and Peter Richtárik. Primal dual interpretation of the proximal stochastic gradient Langevin algorithm. In *Advances in Neural Information Processing Systems (NeurIPS)*, volume 33, 2020.
- [Sta99] Wilhelm Stannat. (Nonsymmetric) Dirichlet operators on  $L^1$ : existence, uniqueness and associated Markov processes. *Annali della Scuola Normale Superiore di Pisa-Classe di Scienze*, 28(1):99–140, 1999.
- [Stu10] Andrew M Stuart. Inverse problems: A Bayesian perspective. *Acta Numerica*, 19:451–559, 2010.
- [Tan79] Hiroshi Tanaka. Stochastic differential equations with reflecting boundary condition in convex regions. *Hiroshima Mathematical Journal*, 9:163–177, 1979.
- [TTV16] Yee Whye Teh, Alexandre H Thiery, and Sebastian J Vollmer. Consistency and fluctuations for stochastic gradient Langevin dynamics. *The Journal of Machine Learning Research*, 17(1):193–225, 2016.
- [Wan97] Feng-Yu Wang. On estimation of the logarithmic Sobolev constant and gradient estimates of heat semigroups. *Probability Theory and Related Fields*, 108:87–101, 1997.
- [WHC14] Sheng-Jhih Wu, Chii-Ruey Hwang, and Moody T. Chu. Attaining the optimal Gaussian diffusion acceleration. *Journal of Statistical Physics*, 155(3):571–590, 2014.

- [ZL22] Yuping Zheng and Andrew Lamperski. Constrained Langevin algorithms with L-mixing external random variables. In *Advances in Neural Information Processing Systems (NeurIPS)*, volume 35, 2022.
- [ZFP20] Kelvin Shuangjian Zhang, Gabriel Peyré, Jalal Fadili, and Marcelo Pereyra. Wasserstein control of mirror Langevin Monte Carlo. In *Conference on Learning Theory*, volume 125, pages 3814–3841. PMLR, 2020.